

Full Research Paper

Modifications of Poly(*o*-phenylenediamine) Permselective Layer on Pt-Ir for Biosensor Application in Neurochemical Monitoring

Sarah M. Kirwan¹, **Gaia Rocchitta**^{1,\$}, **Colm P. McMahon**¹, **Jennifer D. Craig**¹, **Sarah J. Killoran**¹, **Kylie B. O'Brien**^{1,2}, **Pier A. Serra**^{1,\$}, **John P. Lowry**² and **Robert D. O'Neill**^{1,*}

¹ UCD School of Chemistry and Chemical Biology, University College Dublin, Belfield, Dublin 4, Ireland; E-mail: Robert.O'Neill@UCD.ie

² Sensors Development Unit, BioAnalytics Laboratory, Department of Chemistry, National University of Ireland, Maynooth, Co, Kildare, Ireland; E-mail: John.Lowry@NUIM.ie

^{\$} Present Address: Department of Pharmacology, Medical School, University of Sassari, Viale S. Pietro 43/b, 07100, Sassari, Italy

* Author to whom correspondence should be addressed.

Received: 27 March 2007 / Accepted: 10 April 2007 / Published: 12 April 2007

Abstract: Reports that globular proteins could enhance the interference blocking ability of the PPD (poly(*o*-phenylenediamine) layer used as a permselective barrier in biosensor design, prompted this study where a variety of modifying agents were incorporated into PPD during its electrosynthesis on Pt-Ir electrodes. Trapped molecules, including fibrous proteins and β -cyclodextrin, altered the polymer/modifier composite selectivity by affecting the sensitivity to both H₂O₂ (signal molecule in many enzyme-based biosensors) and the archetypal interference species, ascorbic acid. A comparison of electrochemical properties of Pt and a Pt-Ir alloy suggests that the benefits of the latter, more rigid, metal can be exploited in PPD-based biosensor design without significant loss of backward compatibility with studies involving pure Pt.

Keywords: Platinum-iridium electrodes, Polymer electrosynthesis, Cyclic voltammetry, Amperometry, Proteins, Cyclodextrins, Ascorbate, Hydrogen peroxide, Brain analysis.

1. Introduction

Biosensors exploit the specificity of a biological component, such as a cell [1–3] or tissue [1,2,4,5], but usually an enzyme [2,6–10], to provide sensitivity to a target analyte. This chemical specificity can be very high, even to the level of stereoselectivity, for example, the use of L-glutamate oxidase (GluOx) [11] in the design of electrochemical biosensors to detect neurotransmitter L-glutamate (Glu) [8,12–17]. However, the remarkable specificity of enzyme-based amperometric biosensors can be seriously undermined by interference from electroactive species present in the target system, reducing the selectivity of the device. This problem is particularly pronounced for biosensors implanted in biological tissues for real-time monitoring [1,8,10,18–21], because separation techniques cannot be exploited to eliminate the interference, as is the case for on-line microdialysis approaches to *in-vivo* monitoring [22–24]. Despite this drawback, considerable efforts have been made over the past two decades to overcome interference in biosensor signals, mainly because of the significant benefits of biosensor monitoring *in vivo*: small probe size, minimizing tissue damage [25,26]; and sub-second time resolution, allowing real-time correlation with animal behavior [10,18,24].

A number of strategies have been employed to maximize biosensor selectivity. For example, redox mediators have been used to compete with the natural co-substrate of the oxidase enzymes incorporated into most biosensor designs. This avoids the need for oxidation of H₂O₂ at relatively high applied potentials as the electrochemical signal generating step, replacing it with the electrochemical oxidation of the enzyme-reduced mediator at lower potentials; this eliminates interference by species oxidizing more anodically [27–29]. Another strategy involves the use of secondary enzymes to eliminate the interference species before it reaches the electrode surface. The commonest example of this method is the use of ascorbic acid oxidase (AAOx) to convert the ubiquitous biological reducing agent, ascorbic acid (AA; ascorbate at physiological pH), into dehydroascorbate (DHA; see Rxn. 4) [15,30]. The most widespread approach for increasing biosensor selectivity, however, is the incorporation of a permselective membrane into the sensor design to block access of interference molecules to the active electrode surface. Several methods have been devised for the deposition of the permselective barrier, including pre-cast [31], cast [32] and electrosynthesized forms [33,34]. This latter approach has proved most effective, and interference blocking levels for AA greater than 99.9% have been reported using polyphenols [35].

Such levels of AA blocking are often needed for *in-vivo* applications because of the high concentration of AA in many biological tissues [36], and especially in brain extracellular fluid (ECF) which is the most common site of biosensor implantation for neurochemical monitoring [1,24,37–39]. Very low permeability of the membrane to AA, however, often leads to decreases in the response of the biosensor to its target analyte because access of the enzyme transduction molecule, H₂O₂, to the electrode surface is also blocked to some extent [35]. Thus, the value of a particular membrane in biosensor function is better expressed, not in terms of permeability to interference, but as a selectivity parameter [40,41] that incorporates both interference sensitivity and target signal strength [28,42].

Here we investigate a number of modifications of a commonly used interference-rejecting layer, electrosynthesized PPD (poly(*o*-phenylenediamine)), in an attempt to increase further its selectivity for biosensor applications in neurochemical monitoring. The selectivity of existing PPD-based biosensors

for brain glucose is more than adequate [43–45], because the ECF concentration of this important energy metabolite is high (~0.5 mM [46,47]), and of the same order as that of the main interference, AA [36,48]. However, the long-term monitoring of key neurochemicals which have much lower ECF levels, such as Glu (~5 μ M [17,49–51]), requires better selectivity than presently available, and is the motivation for the work reported here.

2. Experimental Section

The overall experimental design involved electrosynthesizing polymers amperometrically, mainly using *o*-phenylenediamine (oPD) as monomer, onto either bare Pt or Pt-Ir wire electrodes. All monomer solutions were buffered at a pH value close to neutrality to obtain the non-conducting form of the respective polymer [52] which has low permeability to interference species, such as AA and urate [33,43,53–55]. Electropolymerizations were also carried out in monomer solutions containing additives, such as albumins, that can affect the permselectivity of the resultant polymer [55]. Amperometric calibrations were then carried out to determine the sensitivity of the modified surface to H₂O₂, the signal molecule in many biosensor designs, where appropriate, and to AA, the archetypal interference present in biological media.

2.1. Instrumentation and Software

Experiments were performed in a standard three-electrode glass electrochemical cell. A saturated calomel electrode (SCE) was used as the reference electrode and a large stainless steel needle served as the auxiliary electrode. Constant potential amperometry was performed at +700 mV using Chart (v5.2) software (AD Instruments Ltd., Oxford, UK), and a low-noise potentiostat (Biostat II, Electrochemical and Medical Systems, Newbury, UK; or Biostat IV, ACM Instruments, Cumbria, UK). A Powerlab/400 interface system (AD Instruments Ltd.) was used to acquire data onto a PC. Cyclic voltammetry was carried out using in-house software written in QuickBasic[®], as described previously [56].

2.2. Reagents and Solutions

The monomers studied in this work were high purity *o*-phenylenediamine (oPD, Sigma Chemical Co.) and 3-methyl-*o*-phenylenediamine (oPD-Me, Aldrich Chemical Co.). L-ascorbic acid (AA) and H₂O₂ (30% w/w aqueous solution) were supplied by Sigma. All chemicals were used as supplied.

Solutions of monomer (300 mM, unless otherwise stated) were made up freshly each time in 25 mL of a phosphate-buffered saline solution (PBS). Stock solutions of 100 mM AA were prepared in 0.01 M HCl prepared from doubly distilled water. Because albumin has been shown to increase the compactness of some electrosynthesised polymers [53,54,57], a variety of agents (from Sigma) were added at a range of concentrations to some monomer solutions to investigate their affect on the polymer formed. These included bovine serum albumin (BSA, Fraction V), chicken egg albumin (CEA, Grade V), gelatine (Type 1, from porcine skin), casein and β -cyclodextrin (CD). Amperometric calibrations (+700 mV) were carried out *in vitro* in PBS (pH 7.4) that consisted of NaCl (BDH, AnalaR

grade, 150 mM), NaH_2PO_4 (BDH, AnalaR grade, 40 mM) and NaOH (Sigma, 40 mM). Solutions were kept refrigerated when not in use.

2.3. Electrode Preparation and Polymer Modification

The main working electrodes used in this study were fabricated using platinum:iridium (90:10) Teflon[®]-insulated wire, bare wire diameter 125 μm (Advent Research Materials, Eynsham, UK). The use of Pt-Ir was favored due to its mechanical rigidity compared to pure Pt, making the wire easier to manipulate during *in-vitro* experiments [55] and for later implantation *in vivo*. Cylinder electrodes were prepared from approximately 4 cm lengths of the coated wire. At one end of the wire approximately 3 mm of Teflon[®] was stripped away using a scalpel to expose the bare wire. This end was soldered into a gold clip for connection to the potentiostat. Approximately 1.5 mm of Teflon[®] was then stripped away from the other end and, using a microscope, the wire was cut down to 1.0 mm \pm 0.1 mm in length.

The stock solutions of monomer (300 mM in PBS, unless stated otherwise) or monomer/modifier mixtures were used in the electropolymerization procedure. Electro-oxidative polymerization was carried out amperometrically for 15 or 30 min at +700 mV vs. SCE to produce the modified electrodes; previous studies revealed little or no difference between PPD films formed for these time periods [54]. Electropolymerization at pH values close to neutrality produces PPD in its non-conducting, self-sealing form which is appropriate for a permselectivity function [33,43,53–55]. Amperometry was chosen as the preferred electropolymerization method, because cyclic voltammetry has been shown to form polymers of greater permeability to certain interfering analytes [58]. The polymer-modified electrodes were stored in PBS at 4 °C when not in use. All polymer modified electrodes were allowed to settle overnight at +700 mV in PBS and calibrations were carried out the following day. The long-term stability of these polymers is not a major issue because effective blocking of AA has been observed several weeks after implantation in brain tissue [59].

2.4. Electrode Characterization and Data Analysis

Bare metal Pt and Pt-Ir wire electrodes were characterized using cyclic voltammetry at 20 mV/s, as described previously for macrodisks [56], and the response converted to current density, using the geometric area of the cylinders ($4.05 \times 10^{-3} \text{ cm}^2$). The double-layer capacitance (Eqn. 1, where v is the scan rate) was determined in PBS at a potential (400 mV) where the anodic and cathodic arms of the voltammograms were essentially horizontal (Figure 1, inset). To quantify the position of a voltammetric wave for an analyte on the potential axis when a peak is not present or is broad, the potential at which the current rises most steeply (potential of maximum slope, $E_{s,\text{max}}$) can be used [60,61]. Differences in $E_{s,\text{max}}$ recorded under similar conditions (scan rate, pH, etc.) reflect differences in electron transfer kinetics (k^0) for a given analyte on different electrodes [60]. There is some debate whether $E_{s,\text{max}}$ or the slope itself (S_{max}) at $E_{s,\text{max}}$ is the better index of electron transfer kinetics [60]. We therefore report both parameters here in order to compare the behavior of Pt and Pt-Ir electrodes effectively. Because S_{max} ($\mu\text{A cm}^{-2} \text{ mV}^{-1}$) also depends on non-geometrically computed aspects of electrode area (e.g., roughness) and the concentration of analyte [56], the value of S_{max} was normalized

with respect to the corresponding current at the reversal potential for each scan, and is represented as $S_{\max,N}$ (mV^{-1}).

$$C_{dl} = \frac{i_{400}(\text{anodic}) - i_{400}(\text{cathodic})}{\nu} \quad (1)$$

The polymer-modified wire electrodes were calibrated amperometrically at 700 mV vs SCE with H_2O_2 and/or AA. The H_2O_2 calibrations were carried out in the range 0 – 0.1 mM, prior to an AA calibration in the range 0 – 1 mM. The H_2O_2 calibration plots of the steady-state responses were linear at all modified surfaces, as reported for previous Pt/PPD electrodes [53,59]; the H_2O_2 sensitivity is therefore reported as the slope (nA mM^{-1} or $\mu\text{A cm}^{-2} \text{mM}^{-1}$) of the calibration. The response of AA at Pt/PPD type electrodes is distinctively non-linear, forming a well-defined plateau at AA concentrations greater than 0.5 mM [42,53,55,59], either hyperbolically or after a relative maximum, $i_{\max}(\text{AA})$, is observed; see Figure 2. This non-linear behavior has been interpreted previously in terms of self-blocking by AA, or its oxidation products, trapped in the polymer matrix [53,55]. The main sensitivity parameter for AA used here was the limiting current at 1 mM, $i_L(\text{AA})$, because brain ECF levels can approach millimolar levels during period of behavioral stimulation [48,62,63]. However, we also used the maximum steady-state current recorded during the AA calibration, $i_{\max}(\text{AA})$, as an additional index of polymer properties.

In the present context, a high response to H_2O_2 is advantageous, and modifications that decreased H_2O_2 sensitivity were generally avoided. However, the selectivity coefficient, S% (Eqn. 2), was the main criterion used for judging the effectiveness of a particular modification. We define S% in terms of the current recorded for 1 mM of each of H_2O_2 , $i(\text{H}_2\text{O}_2)$, and the interference species AA, $i_L(\text{AA})$. The S% value was calculated as the percentage interference, Eqn. 2, because $i_L(\text{AA})$ is very small compared with $i(\text{H}_2\text{O}_2)$ and is ideally zero; thus the optimum value of S% defined in this way is zero [55]. The use of equimolar concentrations in this definition allows S% to be interpreted in terms of the ratio of effective polymer permeability for two analytes with the same z -value (electrons transferred per molecule), as is the case for AA and H_2O_2 ($z = 2$; see Rxns. 3 and 4) [42].

$$S\% = 100 * \frac{i_L(\text{AA})}{i(\text{H}_2\text{O}_2)} \% \quad (2)$$

Values of electrochemical parameters are presented as mean \pm SEM, with n = number of electrodes, unless stated otherwise. The statistical significance of differences observed between responses for the various designs was calculated using Student's two-tailed paired or unpaired t-tests on either the absolute parameter values or on changes expressed as a percentage of the baseline value. Values of $p < 0.05$ were considered to indicate statistical significance of the difference or change.

3. Results and Discussion

3.1. Comparison of Pt and Pt-Ir, using cyclic voltammetry and amperometry

The electrochemical properties of AA and H_2O_2 at Pt-Ir alloy wires [64], used as substrate for the majority of the polymer-modified electrodes described here, were compared directly with those of pure Pt. The characteristics of the cyclic voltammetric response of the two metal types were determined in the background electrolyte (PBS) and in PBS containing either 1 mM H_2O_2 or AA (Figure 1). The basic irreversible electrochemistry of AA on solid electrode surfaces has been described before [53,65–

69], as has that of H_2O_2 [53,64,70,71]. One difference between these two molecules is the ability of H_2O_2 to be electrochemically reduced [53,72], as well as oxidized, an attribute evident in Figure 1.

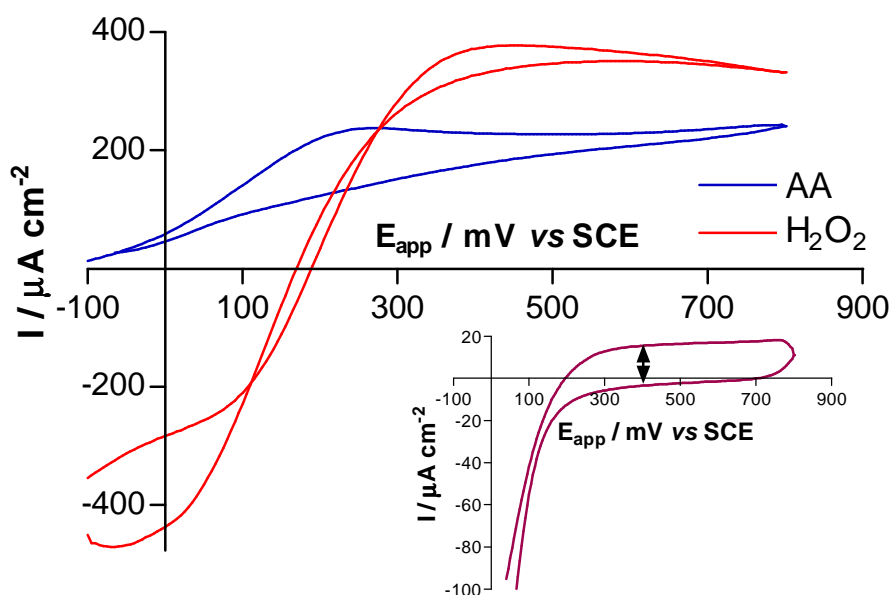


Figure 1. Cyclic voltammograms recorded at 20 mV/s for Pt wire electrodes in PBS containing either 1 mM AA or 1 mM H_2O_2 . The background current, recorded in PBS only, has been subtracted to isolate the Faradaic response of the analytes. *Inset:* background current, recorded in PBS only, showing the potential used to determine the double-layer capacitance (arrow).

First, some of the electrochemical characteristics of the background current, recorded in PBS only, were quantified (see Figure 1 inset, and Table 1). The main contributions to the CV for Pt in PBS are double-layer capacitance and the redox chemistry of metal oxide formation and reduction [73,74]. The shape of the CV for Pt wires in PBS was essentially the same as that for Pt (1.6 mm disks) reported previously [56]. There was no difference in the double-layer capacitance (Eqn. 1; see Figure 1, inset), for the Pt and Pt-Ir electrodes. Taken together with the finding that there was also no significant difference between the background current at the CV reversal potential (oxide formation plateau) for the two metal types, these results indicate that some important characteristics of Pt and Pt-Ir are similar, such as effective surface area (roughness) and metal oxide formation; see Table 1 for statistical comparison. The electrochemistry of H_2O_2 and AA on the two metals was also investigated by cyclic voltammetry (Rxns. 3 and 4). The finding that neither kinetic parameter, $E_{s,\max}$ nor $S_{\max,N}$ (Table 1; see Section 2.4), for both analytes showed any significant difference between Pt and Pt-Ir suggests that the Ir-containing alloy can be used for its greater strength in place of pure Pt, without a major loss of compatibility with previous electrochemical data obtained for Pt-based electrodes.



However, a more direct comparison of the amperometric sensitivity of the two metals was carried out. Because of the key involvement of Pt oxides in H_2O_2 electro-oxidation [75], and because the oxide state of the electrode surface is expected to be different under voltammetric scanning and constant potential conditions [64], the calibration slopes for H_2O_2 and AA were determined on bare Pt and Pt-Ir

electrodes at 700 mV vs. SCE. There was no difference ($p > 0.96$) between the AA slope for pure Pt ($147 \pm 27 \mu\text{A cm}^{-2} \text{mM}^{-1}$, $n = 10$) and the Pt-Ir alloy ($148 \pm 7 \mu\text{A cm}^{-2} \text{mM}^{-1}$, $n = 20$). There was, however, a significant difference ($p < 0.002$) between the calibration slopes for H_2O_2 : Pt ($225 \pm 15 \mu\text{A cm}^{-2} \text{mM}^{-1}$, $n = 8$); Pt-Ir ($171 \pm 6 \mu\text{A cm}^{-2} \text{mM}^{-1}$, $n = 51$), a loss of sensitivity for the alloy compared with the pure metal which is consistent with previous studies [64]. Fortunately, this unwelcome property of Pt-Ir, in the context of H_2O_2 detection for biosensor applications, was reversed by modification with PPD (see Section 3.2). The greater sensitivity of both bare metal electrode types for H_2O_2 compared with AA is in line with diffusion coefficient values for the two analytes [76,77] and diffusion-limited kinetics at 700 mV (see Figure 1).

Table 1. Comparison of electrochemical properties of Pt and Pt-Ir, determined using cyclic voltammetry at 20 mV/s (see Figure 1), in background electrolyte (PBS) and in PBS containing either 1 mM H_2O_2 or 1 mM AA. H_2O_2 and AA parameters were calculated following subtraction of the background current. Number of determinations, n = number of electrodes \times number of scans.

Parameter	Pt	Pt-Ir	<i>p</i> -value
Background scans			
Current at the CV reversal potential ($\mu\text{A cm}^{-2}$); $n = 4 \times 10$	17.4 ± 1.1	16.6 ± 0.9	0.62
Double-layer capacitance, C_{dl} (Eqn. 1; mF cm^{-2}); $n = 4 \times 10$	0.48 ± 0.02	0.45 ± 0.01	0.15
H_2O_2 scans			
Potential of maximum slope ($E_{s,max}$, mV); $n = 2 \times 20$	200 ± 5	195 ± 5	0.55
Normalized maximum slope ($S_{max,N}$, mV^{-1}); $n = 2 \times 20$	0.45 ± 0.01	0.43 ± 0.01	0.30
AA scans			
Potential of maximum slope ($E_{s,max}$, mV); $n = 2 \times 20$	110 ± 5	115 ± 5	0.55
Normalized maximum slope ($S_{max,N}$, mV^{-1}); $n = 2 \times 20$	0.59 ± 0.01	0.51 ± 0.07	0.38

3.2. Comparison of H_2O_2 sensitivity at bare and PPD-modified electrodes

The primary aim of the work reported in this paper was to determine whether modifications of PPD-coated Pt-Ir (Pt-Ir/PPD) could be used to improve the selectivity of the polymer layer for biosensor applications. In principle, this could be achieved in two ways: increase the H_2O_2 sensitivity, or enhance the interference blocking ability of the layer (see Eqn. 2). Evidence that the sensitivity to H_2O_2 for PPD and PPD-enzyme composite electrodes is similar to that for bare metal [42,53,55] indicates, however, that H_2O_2 sensitivity is maximal for the basic design, and that the only strategy available for increased selectivity is reducing the sensitivity to interference. Logically, therefore, only modifications that increased interference blocking needed to be tested for the possibility of decreased H_2O_2 sensitivity; those modifications that give poorer interference blocking can be rejected on that basis alone.

It was important to test rigorously, using a large population of wire electrodes, the hypothesis that ultra-thin (10-30 nm [33,55,78,79]) electrosynthesized PPD does not decrease the sensitivity of Pt-Ir to H_2O_2 [55]. Calibrations for H_2O_2 at Pt-Ir cylinders, before and after PPD modification, were therefore carried out. Surprisingly, this sample size revealed that PPD-modified Pt-Ir showed a small, but statistically significant, increase in the H_2O_2 calibration slope ($189 \pm 10 \mu\text{A cm}^{-2} \text{mM}^{-1}$, $n = 51$) compared with the bare metal ($171 \pm 6 \mu\text{A cm}^{-2} \text{mM}^{-1}$, $n = 51$, $p = 0.05$ for a paired t-test). One

possible explanation for the unexpected increase in the efficiency of the electrochemical H_2O_2 oxidation on the coated metal (see Section 3.1) is that the PPD inhibits the H_2O_2 disproportionation reaction (Rxn. 5) at the electrode surface, the extent of which varies with electrode condition [80]. It is clear, however, that the basic Pt-Ir/PPD design displays near-optimal H_2O_2 sensitivity, so that the only effective way to improve selectivity significantly is to increase interference blocking by the polymer layer.



In the present context, it is interesting to cite the small decrease in H_2O_2 sensitivity observed previously following PPD modification of pure Pt electrodes [53]. Thus, although the decrease was not statistically significant when compared to the bare Pt in the original study, these results indicate a convergence of the H_2O_2 sensitivity for Pt/PPD ($196 \pm 20 \mu\text{A cm}^{-2} \text{mM}^{-1}$, $n = 8$) and Pt-Ir/PPD ($189 \pm 10 \mu\text{A cm}^{-2} \text{mM}^{-1}$, $n = 51$; $p > 0.79$). Pt-Ir working electrodes were therefore used throughout the remainder of the work presented here.

3.3. Comparison of oPD and oPD-Me as monomers

Analysis of AA calibrations reported recently showed that inclusion of a globular protein (BSA) in the monomer oPD solution improved the interference blocking properties of the PPD film formed [55]. The presence of a pronounced $i_{\text{max}}(\text{AA})$ at low concentrations of AA for BSA-free PPD suggested that this polymer was capable of transporting AA, but that this ability diminished significantly as AA/DHA levels built up in the polymer matrix. In an attempt to decrease further the permeability of PPD to hydrophilic ions, such as AA, by adding additional hydrophobicity and steric bulk to the polymer, a methylated derivative of oPD was polymerized onto Pt-Ir in the presence and absence of BSA. Calibrations for AA at these Pt-Ir/PPDMe and Pt-Ir/PPDMe-BSA electrodes are shown in Figure 2, and compared to previously reported data for Pt-Ir/PPD and Pt-Ir/PPD-BSA [55]. Pt-Ir/PPDMe electrodes showed no $i_{\text{max}}(\text{AA})$ peak in the calibration; instead the AA steady-state responses increase monotonically with concentration to the limiting plateau value, $i_{\text{L}}(\text{AA})$, which was not different from that observed for Pt-Ir/PPD ($p > 0.99$). Over the entire calibration, therefore, the methylated polymer was less permeable to AA compared with PPD, as expected. However, the inclusion of BSA in the monomer solution did not enhance the AA blocking ability of PPDMe, with no significant difference between $i_{\text{L}}(\text{AA})$ for Pt-Ir/PPDMe and Pt-Ir/PPDMe-BSA ($p > 0.35$; see Figure 2). The mechanism by which BSA in the monomer solution leads to better interference blocking by the polymer is unknown at present. It is clear from Figure 2 that BSA can improve the permselectivity of PPD, with Pt-Ir/PPD-BSA having the lowest $i_{\text{L}}(\text{AA})$ value of the four electrode types ($p < 0.001$), and 99.8% lower than bare Pt-Ir (~600 nA) [55].

These results are in line with previous reports that BSA does not augment the blocking properties of other polymers, such as polyaniline [55] and polyphenol [35]. The finding here that even the smallest deviation from the oPD structure (methylation) negated the benefits of BSA on the resulting polymer was surprising, and prompted us to investigate the role of BSA in PPD formation further.

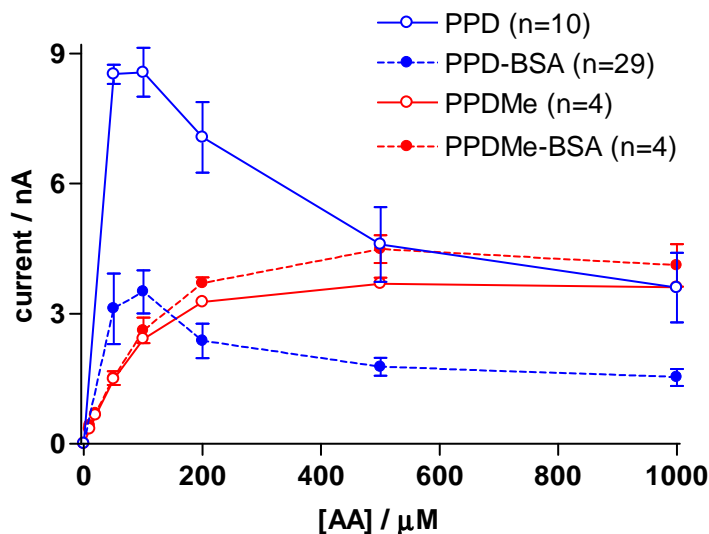


Figure 2. Comparison of steady-state AA calibrations carried out amperometrically on Pt-Ir/PPD, Pt-Ir/PPD-BSA, Pt-Ir/PPDMe and Pt-Ir/PPDMe-BSA electrodes. Data for the PPD systems were taken from the literature [55] for direct comparison with PPDMe.

3.4. Effect of albumins in the monomer solution on resulting polymers

Among the applications envisioned for biosensors are bedside monitoring and other clinical uses [1,81]. The inclusion of a bovine protein in biosensor fabrication for such applications might give rise to problems related to the perception of risks associated with transmissible spongiform encephalopathies (BSE/CJD) [82], which could be avoided by the replacement of BSA. The first step in this section of the work, therefore, was to determine whether other proteins could mimic the effect of BSA on AA rejection by PPD coatings. Table 2 shows that chicken egg albumin (CEA; 45 kDa) had the same effect on all four response parameters as did BSA (66 kDa), when used at the same weight concentration (5 mg/mL) in the oPD solution.

Table 2. AA calibration parameters, H_2O_2 slope and selectivities for PPD formed in oPD solutions containing two different albumins (bovine serum and chicken egg at 5 mg/mL).

Values of p were calculated using unpaired two-tailed t -tests. Number of electrodes in parenthesis.

Albumin	$i_L(\text{AA})$ nA	$i_{\max}(\text{AA})$ nA	H_2O_2 slope nA mM^{-1}	S% (Eqn. 2)
BSA	1.5 ± 0.2 (29)	3.5 ± 0.3 (29)	661 ± 92 (6)	0.23 ± 0.04
CEA	1.6 ± 0.2 (12)	3.1 ± 1.2 (12)	620 ± 10 (8)	0.27 ± 0.03
p-value	$p > 0.74$	$p > 0.69$	$p > 0.61$	$p > 0.43$

Although globular proteins, such as BSA, have been shown to have a marked positive effect on some polymer properties, including surface compactness [53], and AA-rejecting capabilities [53,54,57], the optimum concentration of protein needed to elicit these effects has not been determined

previously. There was no significant effect on S% (Eqn. 2) of increasing the concentration of CEA from 5 mg/mL (Table 2) to 15 mg/mL (0.41 ± 0.15 , $n = 10$, $p > 0.31$), 30 mg/mL (0.33 ± 0.13 , $n = 12$, $p > 0.55$), 50 mg/mL (0.25 ± 0.14 , $n = 8$, $p > 0.82$), or close to saturation at 75 mg/mL (0.41 ± 0.18 , $n = 4$, $p > 0.30$). These results, determined over such a large range of CEA concentration, indicate that the effect of the albumin in the monomer solution is mediated, not through its physicochemical influence on monomer activity or on the solubility of polymerization intermediates (e.g., dimers [83]), but on the protein which is trapped in the polymer as it forms. This latter phenomenon is illustrated by the entrapment of enzyme proteins in the electrosynthesized polymer when these enzymes are included in the oPD solution [59,84]. Furthermore, the results suggest that the maximum amount of CEA is trapped at 5 mg/mL, which is in line with the finding for glucose oxidase [53].

Although a number of groups use low millimolar concentrations of oPD to generate PPD [79,85], we have shown that much higher concentrations provide the level of interference blocking needed for neurochemical monitoring [44,53,54]. Before proceeding to investigate the effects of other modifiers on PPD properties, a detailed comparison was made between PPD formed from 200 and 300 mM oPD, the latter being close to saturation in PBS. All four electrochemical parameters tended to be slightly worse for the PPD-BSA formed from 200 mM oPD, although not statistically different. Most importantly, the S% value tended to be inferior: 0.35 ± 0.06 , $n = 4$, $p = 0.12$). A monomer concentration of 300 mM was maintained, therefore, for the remainder of this work.

3.5. Effect of other modifiers in the monomer solution on resulting polymers

Having shown that different globular proteins, e.g., BSA, CEA and glucose oxidase [53], have similar effects on the selectivity of PPD-modified Pt-Ir, the influence of fibrous proteins was investigated. Gelatin is a protein product formed by the partial hydrolysis of collagen, a fibrous macromolecule found in skin, bones and tendons, and has many uses in food, medicine and manufacturing. Casein is the predominant phosphoprotein in milk, and consists of a fairly high number of proline peptides giving it considerable hydrophobic properties. The effects of these two fibrous proteins, at 5 mg/mL in the oPD solution, on the resulting PPD properties were more pronounced than those of the globular proteins; see Table 3. Thus, although the AA blocking ability of PPD-gelatin were as good as that of PPD-albumin (Table 2), and that of PPD-casein significantly better, both fibrous proteins caused a marked reduction in the sensitivity of the Pt-Ir/PPD electrode to H₂O₂. Overall, the S% was therefore worse for gelatin ($p < 0.001$) and not significantly different for casein ($p > 0.30$). Taking the H₂O₂ sensitivity and S% values in account, modification of PPD with fibrous protein was not considered suitable for biosensor applications.

Cyclodextrins are toroidal cyclic oligosaccharides with a wide variety of applications involving host-guest complexation [86,87] which can be exploited in sensor design [88–90]. The inclusion of β CD at 5 mg/mL in the oPD monomer solution produced a polymer which had excellent AA-rejection properties coupled with high permeability to H₂O₂ (Table 3). The selectivity coefficient, S%, was an improvement on that observed for any other modification of PPD to date, and warranted an investigation of its concentration dependence.

Table 3. AA calibration limiting current, H₂O₂ slope and selectivities for PPD formed in oPD solutions containing different modifiers (each at 5 mg/mL). Values of *p* were calculated using unpaired two-tailed t-tests, comparing S% for each PPD-modifier composite with that for PPD-CEA (Table 2). Number of electrodes in parenthesis.

Modifier	$i_L(\text{AA})$ nA	H ₂ O ₂ slope nA mM ⁻¹	S% (Eqn. 2)	<i>p</i> -value
Gelatin	1.1 ± 0.1 (6)	117 ± 17 (6)	0.90 ± 0.15	<i>p</i> < 0.001
Casein	0.7 ± 0.1 (4)	182 ± 54 (4)	0.37 ± 0.12	<i>p</i> > 0.30
βCD	0.9 ± 0.2 (10)	533 ± 60 (8)	0.17 ± 0.04	<i>p</i> = 0.06

Whereas it is not uncommon to express the concentration of macromolecules in terms of weight, a mole-based unit is more appropriate for species such as βCD. In the context of its use as a modifier in the 300 mM oPD solution, it was decided to use mol%, i.e., 100 *x* moles of βCD per mole of oPD. On this scale, 5 mg/mL is *ca.* 1.5 mol%. Varying the concentration of βCD from 0.5 to 20 mol% caused a systematic change in $i_L(\text{AA})$: the value decreased abruptly to a minimum of 0.9 ± 0.2 nA (10) for 1.5 mol% and thereafter rose steadily to 3 ± 1 nA (2) at 20 mol%. There was no significant change in the linear calibration slope for H₂O₂ over the range of βCD concentrations used here. The resulting S% values are shown in Figure 3; the trend evident in this parameter essentially reflects variations in $i_L(\text{AA})$. The clear minimum in S% (ideal value being zero; see Eqn. 2) observed between 1 and 5 mol% is in contrast with the lack of any variation seen across the large range of albumin concentrations studied (Section 3.4). It is possible, therefore, that the beneficial effects of βCD at low concentrations are due to its entrapment in the PPD matrix, as observed for other modifiers. However, at higher concentrations the deleterious effects may be due to complexation of the oPD and effective lowering of its availability for polymerization. The value of S% observed for 200 mM oPD (0.35 ± 0.06, *n* = 4; see Section 3.4) is consistent with this explanation.

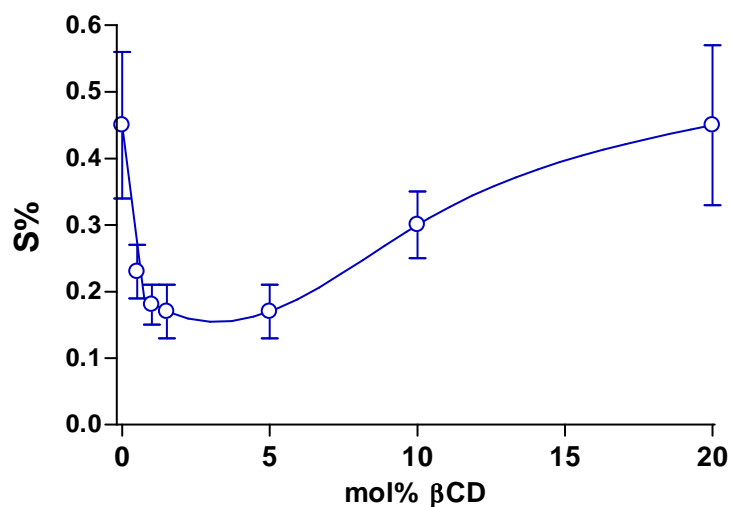


Figure 3. Comparison of the selectivity (S%, Eqn. 2) for Pt-Ir/PPD-βCD sensors electrosynthesized using different concentrations of βCD ranging from 0.5 – 20 mol% in 300 mM oPD.

4. Conclusions

Comparison of cyclic voltammetry data recorded in background electrolyte (PBS) alone, and in PBS containing either AA or H₂O₂ showed that a 90:10 Pt-Ir alloy exhibited a range of similar electrochemical properties to those of pure Pt (Table 1). Although the two bare metals displayed the same amperometric sensitivity for AA, that for H₂O₂ was somewhat lower at Pt-Ir electrodes. Polymer modification, however, led to convergence of the H₂O₂ sensitivity at Pt/PPD and Pt-Ir/PPD. The benefits of the greater rigidity of the alloy can therefore be exploited for implantation of sensors into biological tissues, without significant loss of backward compatibility with studies involving Pt.

A range of selectivity values (S%, Eqn. 2) for PPD-modified Pt-Ir wire electrodes were observed following incorporation of one of a number of proteins into the polymer matrix. Globular proteins (Table 2) generally enhanced the interference rejection properties of the polymer, without affecting H₂O₂ sensitivity significantly. Fibrous proteins, on the other hand, had a greater effect on polymer permeability, reducing it for both AA and H₂O₂ (Table 3). As a result, PPD modified with either gelatin or casein displayed poorer S% values compared with those for the globular polypeptide modifiers. The inclusion of β CD at a concentration between 1 and 5 mol% in the monomer solution gave rise to a PPD composite that displayed ~25% enhanced selectivity compared with the best globular protein value, a finding which should prove useful in the design of biosensors for neurochemical monitoring of analytes with low ECF concentrations.

Acknowledgements

This work was funded in part by Science Foundation Ireland (03/IN3/B376 and 04/BR/C0198), and by the Health Research Board, Ireland (RP/2004/44).

References and Notes

1. Wilson, G.S.; Gifford, R. Biosensors for real-time in vivo measurements. *Biosens. Bioelectron.* **2005**, *20*, 2388-2403.
2. Gorton, L. Carbon paste electrodes modified with enzymes, tissues, and cells. *Electroanalysis* **1995**, *7*, 23-45.
3. Shear, J.B.; Fishman, H.A.; Allbritton, N.L.; Garigan, D.; Zare, R.N.; Scheller, R.H. Single cells as biosensors for chemical separations. *Science* **1994**, *267*, 74-77.
4. Raoof, J.B.; Ojani, R.; Kiani, A. Apple-modified carbon paste electrode: A biosensor for selective determination of dopamine in pharmaceutical formulations. *Bull. Electrochem.* **2005**, *21*, 223-228.
5. Wang, J.; Wu, L.H.; Martinez, S.; Sanchez, J. Tissue bioelectrode for eliminating protein interferences. *Anal. Chem.* **1991**, *63*, 398-400.
6. Bernhardt, P.V. Enzyme Electrochemistry - Biocatalysis on an electrode. *Aust. J. Chem.* **2006**, *59*, 233-256.
7. Zhang, M.N.; Mao, L.Q. Enzyme-based amperometric biosensors for continuous and on-line monitoring of cerebral extracellular microdialysate. *Front. Biosci.* **2005**, *10*, 345-352.

8. Wilson, G.S.; Hu, Y.B. Enzyme based biosensors for in vivo measurements. *Chem. Rev.* **2000**, *100*, 2693-2704.
9. Ikeda, T. Enzyme-modified electrodes with bioelectrocatalytic function (review). *Bunseki Kagaku* **1995**, *44*, 333-354.
10. O'Neill, R.D.; Lowry, J.P.; Mas, M. Monitoring brain chemistry *in vivo*: voltammetric techniques, sensors and behavioral applications. *Crit. Rev. Neurobiol.* **1998**, *12*, 69-127.
11. Kusakabe, H.; Midorikawa, Y.; Fujishima, T.; Kuninaka, A.; Yoshino, H. Purification and properties of a new enzyme, L-glutamate oxidase, from *Streptomyces* sp. X-119-6 grown on wheat bran. *Agric. Biol. Chem.* **1983**, *47*, 1323-1328.
12. McMahon, C.P.; Rocchitta, G.; Kirwan, S.M.; Killoran, S.J.; Serra, P.A.; Lowry, J.P.; O'Neill, R.D. Oxygen tolerance of an implantable polymer/enzyme composite glutamate biosensor displaying polycation-enhanced substrate sensitivity. *Biosens. Bioelectron.* **2007**, *22*, 1466-1473.
13. Hamdi, N.; Wang, J.J.; Walker, E.; Maidment, N.T.; Monbouquette, H.G. An electroenzymatic L-glutamate microbiosensor selective against dopamine. *J. Electroanal. Chem.* **2006**, *591*, 33-40.
14. McMahon, C.P.; Rocchitta, G.; Serra, P.A.; Kirwan, S.M.; Lowry, J.P.; O'Neill, R.D. Control of the oxygen dependence of an implantable polymer/enzyme composite biosensor for glutamate. *Anal. Chem.* **2006**, *78*, 2352-2359.
15. Oldenzien, W.H.; Dijkstra, G.; Cremers, T.I.F.H.; Westerink, B.H.C. Evaluation of hydrogel-coated glutamate microsensors. *Anal. Chem.* **2006**, *78*, 3366-3378.
16. Kulagina, N.V.; Shankar, L.; Michael, A.C. Monitoring glutamate and ascorbate in the extracellular space of brain tissue with electrochemical microsensors. *Anal. Chem.* **1999**, *71*, 5093-5100.
17. Day, B.K.; Pomerleau, F.; Burmeister, J.J.; Huettl, P.; Gerhardt, G.A. Microelectrode array studies of basal and potassium-evoked release of L-glutamate in the anesthetized rat brain. *J. Neurochem.* **2006**, *96*, 1626-1635.
18. Lowry, J.P.; O'Neill, R.D. Neuroanalytical chemistry *in vivo* using electrochemical sensors. In *Encyclopedia of Sensors*; Grimes, C.A.; Dickey, E.C.; Pishko, M.V. (Eds.), American Scientific Publishers, California, **2006**; pp. 501-524.
19. Dale, N.; Hatz, S.; Tian, F.M.; Llaudet, E. Listening to the brain: microelectrode biosensors for neurochemicals. *Trends Biotechnol.* **2005**, *23*, 420-428.
20. Pantano, P.; Kuhr, W.G. Enzyme-modified microelectrodes for in vivo neurochemical measurements. *Electroanalysis* **1995**, *7*, 405-416.
21. Wang, J. Electroanalysis and biosensors. *Anal. Chem.* **1995**, *67*, R487-R492.
22. Ao, X.P.; Stenken, J.A. Microdialysis sampling of cytokines. *Methods* **2006**, *38*, 331-341.
23. Watson, C.J.; Venton, B.J.; Kennedy, R.T. In vivo measurements of neurotransmitters by microdialysis sampling. *Anal. Chem.* **2006**, *78*, 1391-1399.
24. Fillenz, M. In vivo neurochemical monitoring and the study of behaviour. *Neurosci. Biobehav. Rev.* **2005**, *29*, 949-962.

25. Duff, A.; O'Neill, R.D. Effect of probe size on the concentration of brain extracellular uric acid monitored with carbon paste electrodes. *J. Neurochem.* **1994**, *62*, 1496-1502.
26. O'Neill, R.D.; Gonzalez-Mora, J.L.; Boutelle, M.G.; Ormonde, D.E.; Lowry, J.P.; Duff, A.; Fumero, B.; Fillenz, M.; Mas, M. Anomalous high concentrations of brain extracellular uric acid detected with chronically implanted probes: implications for *in vivo* sampling techniques. *J. Neurochem.* **1991**, *57*, 22-29.
27. Calvo, E.J.; Etchenique, R.; Danilowicz, C.; Diaz, L. Electrical communication between electrodes and enzymes mediated by redox hydrogels. *Anal. Chem.* **1996**, *68*, 4186-4193.
28. El Atrash, S.S.; O'Neill, R.D. Characterisation *in vitro* of a naphthoquinone-mediated glucose oxidase-modified carbon paste electrode designed for neurochemical analysis *in vivo*. *Electrochim. Acta* **1995**, *40*, 2791-2797.
29. Kulys, J.; Wang, L.; Hansen, H.E.; Buchrasmussen, T.; Wang, J.; Ozsoz, M. Methylene-green-mediated carbon paste glucose biosensor. *Electroanalysis* **1995**, *7*, 92-94.
30. Nagy, G.; Rice, M.E.; Adams, R.N. A new type of enzyme electrode: the ascorbic acid eliminator electrode. *Life Sci.* **1982**, *31*, 2611-2616.
31. Sternberg, R.; Bindra, D.S.; Wilson, G.S.; Thevenot, D.R. Covalent enzyme coupling on cellulose acetate membranes for glucose sensor development. *Anal. Chem.* **1988**, *60*, 2781-2786.
32. Fan, Z.H.; Harrison, D.J. Permeability of glucose and other neutral species through recast perfluorosulfonated ionomer films. *Anal. Chem.* **1992**, *64*, 1304-1311.
33. Malitesta, C.; Palmisano, F.; Torsi, L.; Zambonin, P.G. Glucose fast-response amperometric sensor based on glucose oxidase immobilized in an electropolymerized poly(o-phenylenediamine) film. *Anal. Chem.* **1990**, *62*, 2735-2740.
34. Ohnuki, Y.; Matsuda, H.; Ohsaka, T.; Oyama, N. Permselectivity of films prepared by electrochemical oxidation of phenol and amino-aromatic compounds. *J. Electroanal. Chem.* **1983**, *158*, 55-67.
35. Craig, J.D.; O'Neill, R.D. Electrosynthesis and permselective characterisation of phenol-based polymers for biosensor applications. *Anal. Chim. Acta* **2003**, *495*, 33-43.
36. Grunewald, R.A. Ascorbic acid in the brain. *Brain Res. Rev.* **1993**, *18*, 123-133.
37. Wightman, R.M. Probing cellular chemistry in biological systems with microelectrodes. *Science* **2006**, *311*, 1570-1574.
38. Bolger, F.B.; Lowry, J.P. Brain tissue oxygen: *in vivo* monitoring with carbon paste electrodes. *Sensors* **2005**, *5*, 473-487.
39. O'Neill, R.D. Long-term monitoring of brain dopamine metabolism *in vivo* with carbon paste electrodes. *Sensors* **2005**, *5*, 317-342.
40. Macca, C.; Wang, J. Experimental procedures for the determination of amperometric selectivity coefficients. *Anal. Chim. Acta* **1995**, *303*, 265-274.
41. Wang, J. Selectivity coefficients for amperometric sensors. *Talanta* **1994**, *41*, 857-863.
42. McMahan, C.P.; Killoran, S.J.; Kirwan, S.M.; O'Neill, R.D. The selectivity of electrosynthesised polymer membranes depends on the electrode dimensions: implications for biosensor applications. *J. Chem. Soc. Chem. Commun.* **2004**, 2128-2130.

43. Schuvailo, O.M.; Soldatkin, O.O.; Lefebvre, A.; Cespuglio, R.; Soldatkin, A.P. Highly selective microbiosensors for in vivo measurement of glucose, lactate and glutamate. *Anal. Chim. Acta* **2006**, *573*, 110-116.
44. Dixon, B.M.; Lowry, J.P.; O'Neill, R.D. Characterization *in vitro* and *in vivo* of the oxygen dependence of an enzyme/polymer biosensor for monitoring brain glucose. *J. Neurosci. Meth.* **2002**, *119*, 135-142.
45. Lowry, J.P.; Miele, M.; O'Neill, R.D.; Boutelle, M.G.; Fillenz, M. An amperometric glucose-oxidase/poly(o-phenylenediamine) biosensor for monitoring brain extracellular glucose: *in vivo* characterisation in the striatum of freely-moving rats. *J. Neurosci. Meth.* **1998**, *79*, 65-74.
46. Lowry, J.P.; O'Neill, R.D.; Boutelle, M.G.; Fillenz, M. Continuous monitoring of extracellular glucose concentrations in the striatum of freely moving rats with an implanted glucose biosensor. *J. Neurochem.* **1998**, *70*, 391-396.
47. McNay, E.C.; McCarty, R.C.; Gold, P.E. Fluctuations in brain glucose concentration during behavioral testing: Dissociations between brain areas and between brain and blood. *Neurobiol. Learn. Memory* **2001**, *75*, 325-337.
48. Miele, M.; Fillenz, M. In vivo determination of extracellular brain ascorbate. *J. Neurosci. Meth.* **1996**, *70*, 15-19.
49. Oldenzel, W.H.; Dijkstra, G.; Cremers, T.I.F.H.; Westerink, B.H.C. In vivo monitoring of extracellular glutamate in the brain with a microsensor. *Brain Res.* **2006**, *1118*, 34-42.
50. Baker, D.A.; Xi, Z.X.; Shen, H.; Swanson, C.J.; Kalivas, P.W. The origin and neuronal function of in vivo nonsynaptic glutamate. *J. Neurosci.* **2002**, *22*, 9134-9141.
51. Miele, M.; Berners, M.; Boutelle, M.G.; Kusakabe, H.; Fillenz, M. The determination of the extracellular concentration of brain glutamate using quantitative microdialysis. *Brain Res.* **1996**, *707*, 131-133.
52. De Giglio, E.; Losito, I.; Torsi, L.; Sabbatini, L.; Zambonin, P.G. Electroanalytical and spectroscopic characterization of poly(o-phenylenediamine) grown on highly oriented pyrolytic graphite. *Annali Chim.* **2003**, *93*, 209-221.
53. Lowry, J.P.; O'Neill, R.D. Partial characterization *in vitro* of glucose oxidase-modified poly(phenylenediamine)-coated electrodes for neurochemical analysis *in vivo*. *Electroanalysis* **1994**, *6*, 369-379.
54. Ryan, M.R.; Lowry, J.P.; O'Neill, R.D. Biosensor for neurotransmitter L-glutamic acid designed for efficient use of L-glutamate oxidase and effective rejection of interference. *Analyst* **1997**, *122*, 1419-1424.
55. Craig, J.D.; O'Neill, R.D. Comparison of simple aromatic amines for electrosynthesis of permselective polymers in biosensor fabrication. *Analyst* **2003**, *128*, 905-911.
56. O'Neill, R.D.; Chang, S.C.; Lowry, J.P.; McNeil, C.J. Comparisons of platinum, gold, palladium and glassy carbon as electrode materials in the design of biosensors for glutamate. *Biosens. Bioelectron.* **2004**, *19*, 1521-1528.
57. McAteer, K.; O'Neill, R.D. Strategies for decreasing ascorbate interference at glucose oxidase-modified poly(o-phenylenediamine)-coated electrodes. *Analyst* **1996**, *121*, 773-777.

58. Centonze, D.; Malitesta, C.; Palmisano, F.; Zambonin, P.G. Permeation of solutes through an electropolymerized ultrathin poly-o-phenylenediamine film used as an enzyme-entrapping membrane. *Electroanalysis* **1994**, *6*, 423-429.
59. Lowry, J.P.; McAteer, K.; El Atrash, S.S.; Duff, A.; O'Neill, R.D. Characterization of glucose oxidase-modified poly(phenylenediamine)-coated electrodes *in vitro* and *in vivo*: homogeneous interference by ascorbic acid in hydrogen peroxide detection. *Anal. Chem.* **1994**, *66*, 1754-1761.
60. Oldham, K.B. The steepness of voltammetric waves. *J. Electroanal. Chem.* **1985**, *184*, 257-267.
61. Lyne, P.D.; O'Neill, R.D. Stearate-modified carbon paste electrodes for detecting dopamine *in vivo*: decrease in selectivity caused by lipids and other surface-active agents. *Anal. Chem.* **1990**, *62*, 2347-2351.
62. O'Neill, R.D. Microvoltammetric techniques and sensors for monitoring neurochemical dynamics *in vivo* - a review. *Analyst* **1994**, *119*, 767-779.
63. O'Neill, R.D.; Grunewald, R.A.; Fillenz, M.; Albery, W.J. The effect of unilateral cortical lesions on the circadian changes in rat striatal ascorbate and homovanillic acid levels measured *in vivo* using voltammetry. *Neurosci. Lett.* **1983**, *42*, 105-110.
64. Zhang, Y.; Wilson, G.S. Electrochemical oxidation of H₂O₂ on Pt and Pt + Ir electrodes in physiological buffer and its applicability to H₂O₂-based biosensors. *J. Electroanal. Chem.* **1993**, *345*, 253-271.
65. Casella, I.G. Electrooxidation of ascorbic acid on the dispersed platinum glassy carbon electrode and its amperometric determination in flow injection analysis. *Electroanalysis* **1996**, *8*, 128-134.
66. Deakin, M.R.; Kovach, P.M.; Stutts, K.J.; Wightman, R.M. Heterogeneous mechanisms of the oxidation of catechols and ascorbic acid at carbon electrodes. *Anal. Chem.* **1986**, *58*, 1474-1480.
67. Hu, I.F.; Kuwana, T. Oxidative mechanism of ascorbic acid at glassy carbon electrodes. *Anal. Chem.* **1986**, *58*, 3235-3239.
68. Evans, J.F.; Kuwana, T.; Henne, M.T.; Royer, G.P. Electrocatalysis of solution species using modified electrodes. *J. Electroanal. Chem.* **1977**, *80*, 409-416.
69. Ormonde, D.E.; O'Neill, R.D. Altered response of carbon paste electrodes after contact with brain tissue. Implications for modified electrode use *in vivo*. *J. Electroanal. Chem.* **1989**, *261*, 463-469.
70. Hall, S.B.; Khudaish, E.A.; Hart, A.L. Electrochemical oxidation of hydrogen peroxide at platinum electrodes. Part 1. An adsorption-controlled mechanism. *Electrochim. Acta* **1998**, *43*, 579-588.
71. Aoki, K.; Ishida, M.; Tokuda, K. Electrode kinetics of the oxidation of hydrogen peroxide at pretreated glassy carbon and carbon fibre electrodes. *J. Electroanal. Chem.* **1988**, *251*, 63-71.
72. Wang, J.; Rivas, G.; Chicharro, M. Iridium-dispersed carbon paste enzyme electrodes. *Electroanalysis* **1996**, *8*, 434-437.

73. Yang, Y.F.; Denuault, G. Scanning electrochemical microscopy (SECM): study of the formation and reduction of oxides on platinum electrode surfaces in Na₂SO₄ solution (pH=7). *J. Electroanal. Chem.* **1998**, *443*, 273-282.
74. Burke, L.D.; Buckley, D.T. Formation and reduction of hydrous oxide films on platinum in aqueous solution at 273 K. *J. Appl. Electrochem.* **1995**, *25*, 913-922.
75. Lingane, J.J.; Lingane, P.J. Chronopotentiometry of hydrogen peroxide with a platinum wire electrode. *J. Electroanal. Chem.* **1963**, *5*, 411-419.
76. Mikkelsen, S.R.; Lennox, R.B. Rotating disc electrode characterization of immobilized glucose oxidase. *Anal. Biochem.* **1991**, *195*, 358-363.
77. Ormonde, D.E.; O'Neill, R.D. The oxidation of ascorbic acid at carbon paste electrodes. Modified response following contact with surfactant, lipid and brain tissue. *J. Electroanal. Chem.* **1990**, *279*, 109-121.
78. Sohn, T.W.; Stoecker, P.W.; Carp, W.; Yacynych, A.M. Microarray electrodes as biosensors. *Electroanalysis* **1991**, *3*, 763-766.
79. Myler, S.; Eaton, S.; Higson, S.P.J. Poly(o-phenylenediamine) ultra-thin polymer-film composite membranes for enzyme electrodes. *Anal. Chim. Acta* **1997**, *357*, 55-61.
80. Harrar, J.E. Controlled-potential coulometric determination of hydrogen peroxide. *Anal. Chem.* **1963**, *35*, 893-896.
81. Jones, D.A.; Parkin, M.C.; Langemann, H.; Landolt, H.; Hopwood, S.E.; Strong, A.J.; Boutelle, M.G. On-line monitoring in neurointensive care - Enzyme-based electrochemical assay for simultaneous, continuous monitoring of glucose and lactate from critical care patients. *J. Electroanal. Chem.* **2002**, *538*, 243-252.
82. Collinge, J.; Sidle, K.C.L.; Meads, J.; Ironside, J.; Hill, A.F. Molecular analysis of prion strain variation and the aetiology of 'new variant' CJD. *Nature* **1996**, *383*, 685-690.
83. Losito, I.; Palmisano, F.; Zambonin, P.G. o-Phenylenediamine electropolymerization by cyclic voltammetry combined with electrospray ionization-ion trap mass spectrometry. *Anal. Chem.* **2003**, *75*, 4988-4995.
84. Cooper, J.M.; Foreman, P.L.; Glidle, A.; Ling, T.W.; Pritchard, D.J. Glutamate oxidase enzyme electrodes: microsensors for neurotransmitter determination using electrochemically polymerized permselective films. *J. Electroanal. Chem.* **1995**, *388*, 143-149.
85. Murphy, L.J. Reduction of interference response at a hydrogen peroxide detecting electrode using electropolymerized films of substituted naphthalenes. *Anal. Chem.* **1998**, *70*, 2928-2935.
86. Schofield, W.C.E.; McGettrick, J.D.; Badyal, J.P.S. A substrate-independent approach for cyclodextrin functionalized surfaces. *J. Phys. Chem. B* **2006**, *110*, 17161-17166.
87. Duo, J.; Fletcher, H.; Stenzen, J.A. Natural and synthetic affinity agents as microdialysis sampling mass transport enhancers: Current progress and future perspectives. *Biosens. Bioelectron.* **2006**, *22*, 449-457.
88. Ferancova, A.; Labuda, J.; Barek, J.; Zima, J. Cyclodextrins as supramolecular complex agents in electroanalytical chemistry: Review 1995-2001. *Chem. Listy* **2002**, *96*, 856-862.

89. Ferancova, A.; Korgova, E.; Labuda, J.; Zima, J.; Barek, J. Cyclodextrin modified carbon paste based electrodes as sensors for the determination of carcinogenic polycyclic aromatic amines. *Electroanalysis* **2002**, *14*, 1668-1673.
90. Ganjali, M.R.; Norouzi, P.; Rezapour, M.; Faridbod, F.; Pourjavid, M.R. Supramolecular based membrane sensors. *Sensors* **2006**, *6*, 1018-1086.

© 2007 by MDPI (<http://www.mdpi.org>). Reproduction is permitted for noncommercial purposes.